

Continuum model of strong light-matter coupling for molecular polaritons

Suman Gunasekaran*, Ryan F. Pinard, and Andrew J. Musser

Department of Chemistry and Chemical Biology, Cornell University, Ithaca, New York 14853

*E-mail: sg875@cornell.edu

ABSTRACT

Strong coupling between light and matter generates hybrid polaritons. We present a continuum model that describes the polaritons by light and matter densities of states (DOS) that only depend on the refractive index of the material. This model is applied to molecular polaritons derived from molecules with broad spectral absorption. While the photonic DOS has a complex spectral distribution, the matter DOS is largely unmodified by strong coupling. We argue that bright states cannot be partitioned from dark states, and instead the photonic DOS is shared over a vast number of matter states.

INTRODUCTION

Strong coupling between the electromagnetic field of an optical cavity and the polarization field of an absorbing material produces hybridized light-matter states known as polaritons.^{1,2} The light-matter interaction for polaritons is typically described by a coupled oscillator model, derived from the Jaynes- or Tavis-Cummings Hamiltonians,^{3,4} which consider a fully quantized light-matter interaction between the cavity photon and the excitation of the material (exciton, phonon etc.). Such coupled oscillator models provide the essential language of polaritons. Meanwhile, experimental scattering measurements of polaritons, that probe the linear light-matter interaction, are primarily sensitive to the frequency-dependent refractive index of the material.⁵ Surprisingly, a generalized relationship between the refractive index and the coupled oscillator model has not been developed. This poses significant limitations to polariton theories when applied to materials, such as organic molecules, with refractive indices derived from manifold absorbing states.

Organic molecules are intricate photophysical systems that feature rich absorption spectra arising from overlapping (vibronic) absorption bands and spectral broadening due to structural disorder. Recently, there has been significant interest in elucidating the behavior of organic molecules in the strong light-matter coupling regime.⁶ Typically, strong coupling is achieved in a Fabry-Perot cavity that is tuned to either an electronic or vibrational transition of the molecules, forming molecular exciton- or vibrational-polaritons, respectively. Molecular polaritons have revealed remarkable properties including enhanced energy⁷⁻⁹ and charge transport,^{10,11} polariton lasing at room temperature,^{12,13} and intriguingly, the ability to undergo chemical reactions at altered rates.¹⁴⁻¹⁶ While the complex photophysics of organic molecules makes molecular polaritons scientifically interesting, it also poses difficulties to existing polariton theories, which were developed for pristine systems such as ultracold atoms¹⁷ and semiconductor quantum wells.¹⁸

Due to a lack of proper theoretical tools, measurements of molecular polaritons are typically fit to simplified coupled oscillator models which do not accurately capture the underlying light-matter interaction. As a result, incorrect conclusions are drawn regarding the polariton states in these systems, which for example affects the interpretation of polariton-enhanced energy/charge transport or polariton-mediated chemistry. Indeed, recent attempts to explicitly incorporate the effects of disorder suggest a fundamental change to the nature of the states formed under strong light-matter coupling and attendant alterations to energy transport and relaxation pathways.^{19,20}

In this letter, we derive a general relationship between the refractive index and the coupled oscillator model. The essence of our approach is to define the polaritons by a continuous density of states (DOS).^{21,22} This perspective is a notable departure from polariton orthodoxy. Though there has been some work on inhomogeneous broadening,^{23–25} polaritons are almost exclusively regarded as discrete, homogeneously broadened states. By instead expressing the polaritons by a continuous DOS, we derive a crucial relationship between the polariton DOS and the refractive index of the material. This allows us to extend the applicability of the coupled oscillator model to polariton states in any material with an arbitrary refractive index. And since the refractive index can be obtained empirically, our derivation establishes an essential bridge between polariton theory and experiment.

RESULTS

We consider N molecular oscillators, with a distribution of frequencies $D(\omega)$, that are coupled to a single photonic mode of an optical cavity. Within the rotating wave approximation, the light-matter interaction is described by a matrix of the following form

$$H = \begin{pmatrix} \tilde{\omega}_0 & V_1 & V_2 & \dots \\ V_1^* & \tilde{\omega}_1 & 0 & 0 \\ V_2^* & 0 & \tilde{\omega}_2 & 0 \\ \vdots & 0 & 0 & \ddots \end{pmatrix}, \quad (1)$$

where $\tilde{\omega}_0 = \omega_0 - i\gamma_0/2$ is the resonant frequency of the cavity, $\tilde{\omega}_j = \omega_j - i\gamma_j/2$ for $j = 1, 2, 3, \dots, N$ are the resonance frequencies of the molecular oscillators, and V_j is the light-matter coupling. The spectrum of H is given by the poles of the Green's matrix: $G(\omega) = \lim_{\eta \rightarrow 0^+} [(\omega + i\eta)I - H]^{-1}$, and the light and matter components of the polariton can be described by densities of states (DOS). The light and matter DOS are the essential quantities we will analyze.

Eq. 1 is closely related to the model of adsorption developed by Newns,²⁶ Anderson,²⁷ and Grimely.²⁸ Following their analysis, the local DOS of basis state m is $\rho_m(\omega) = -\frac{1}{\pi} \text{Im}[G_{mm}(\omega)]$, where $G_{mm}(\omega) = 1/(\omega - \tilde{\omega}_m - \Sigma_m)$ is the (m, m) element of $G(\omega)$, and $\Sigma_m(\omega)$ is the self-energy of state m . Here, $m = 0$ (or subscript *ph*) denotes the photonic state, and $m = j$ denotes a molecular state. For N molecular states, with distribution $D(\omega)$, the self-energy of the photonic state is

$$\Sigma_0(\omega) = \sum_j \frac{|V_j|^2}{\omega - \tilde{\omega}_j} = \int_{-\infty}^{\infty} d\omega_j D(\omega_j) \frac{N|V_j|^2}{\omega - \tilde{\omega}_j}, \quad (2)$$

and the self-energy for matter state j is

$$\Sigma_j(\omega) = |V_j|^2 \left(\omega - \tilde{\omega}_0 - \Sigma_0(\omega) + \frac{|V_j|^2}{\omega - \tilde{\omega}_j} \right)^{-1}. \quad (3)$$

Eq. 3 resembles Eq. 2, but since state j only couples to the photonic state (i.e., state 0), there is only a single term in the summation. This term invokes the effective frequency of the photonic

state, $\tilde{\omega}_0^{eff} = \tilde{\omega}_0 + \Sigma_0(\omega)$, but excludes the contribution to $\Sigma_0(\omega)$ from state j , since state j cannot couple to itself. Using Eq. 3, $G_{jj}(\omega)$ can be expressed in an alternative form,²⁷ where the perturbation due to light-matter coupling is separated from the unperturbed term:

$$G_{jj}(\omega) = \frac{1}{\omega - \tilde{\omega}_j} + G_{00}(\omega) \frac{|V_j|^2}{(\omega - \tilde{\omega}_j)^2}. \quad (4)$$

Research on molecular polaritons is often motivated by an interest in modifying the matter DOS by strong coupling, for instance to modify chemical reactivity. The total matter DOS, which we will denote $\rho_{ex}(\omega)$, is obtained by integrating $\rho_j(\omega)$ over all states j . The subscript *ex* denotes excitation, which can be of any flavor (exciton, phonon, etc.). The total matter DOS can be expressed as $\rho_{ex}(\omega) = \rho_{ex}^0(\omega) + \Delta\rho_{ex}(\omega)$, where $\rho_{ex}^0(\omega)$ is the unperturbed DOS, derived from the first term in Eq. 4, and $\Delta\rho_{ex}(\omega)$ is the change in DOS due to light matter coupling, derived from the second term in Eq. 4. Both $\rho_{ex}^0(\omega)$ and $\Delta\rho_{ex}(\omega)$ can be expressed in simple forms. The term $\rho_{ex}^0(\omega)$ is given by

$$\rho_{ex}^0(\omega) = -\frac{1}{\pi} \text{Im} \int_{-\infty}^{\infty} d\omega_j \frac{ND(\omega_j)}{\omega - \tilde{\omega}_j} \approx ND(\omega), \quad (5)$$

where the approximation represents the limit that $\gamma_j \rightarrow 0$ for all j . From an experimental perspective, $\rho_{ex}^0(\omega)$ is a somewhat ambiguous quantity since N is exceedingly large in typical cavities. In contrast, $\Delta\rho_{ex}(\omega)$ does not depend on N in the same way as $\rho_{ex}^0(\omega)$. Using Eq. 2, $\Delta\rho_{ex}(\omega)$ can be expressed as^{21,29}

$$\Delta\rho_{ex}(\omega) = \frac{1}{\pi} \text{Im} \left[G_{00}(\omega) \frac{d\Sigma_0}{d\omega} \right]. \quad (6)$$

In Eq. 6, N in the numerator of $\Sigma_0(\omega)$ is offset by N in the denominator of $G_{00}(\omega)$. Thus, $\Delta\rho_{ex}(\omega)$, which describes the influence of light-matter coupling, is small compared to $\rho_{ex}^0(\omega)$ for large N . This is the so-called large N problem,³⁰ which is a key distinction between the matter DOS and the photonic DOS.

In Fig. 1, we contrast the conventional discrete polariton picture with the DOS picture that we present. We first consider N degenerate molecular states, with resonance frequency $\tilde{\omega}_j$, that strongly couple to a perfectly resonant cavity mode ($\tilde{\omega}_0 = \tilde{\omega}_j$). The associated matrix H (Eq. 1) can be block diagonalized such that there is a single collective bright matter state with light-matter coupling strength $g = V_j\sqrt{N}$, leaving $N - 1$ collective dark states that are uncoupled. In this basis, the coupling between the bright matter state and the photonic state results in an upper polariton state (UP) and a lower polariton state (LP) with a Rabi splitting of $\Omega = 2g$ (Fig. 1a).

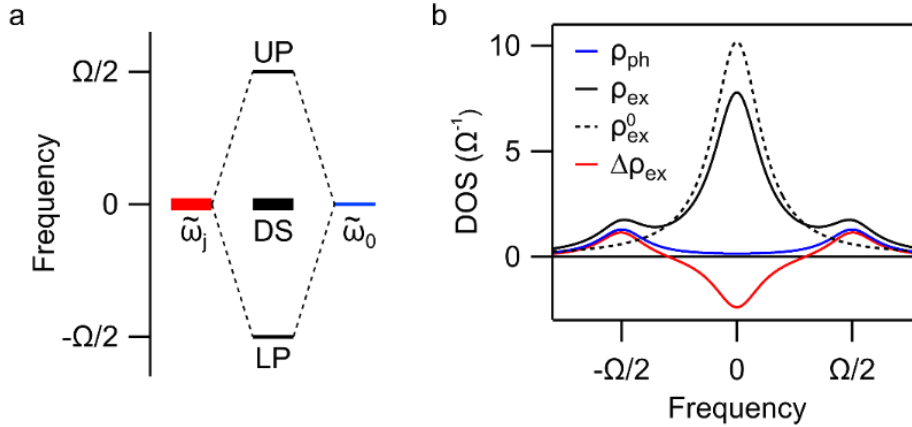


Figure 1. a) Canonical polariton model with Rabi splitting Ω . Strong coupling between a cavity mode ($\tilde{\omega}_0$) and N degenerate absorbers ($\tilde{\omega}_j$) results in UP, LP, and $N - 1$ dark states (DS). b) The photonic DOS (blue) and matter DOS (black) for the continuum model corresponding to (a). The UP and LP states cannot be separated from the total DOS (black) if the originating matter states are nondegenerate. Moreover, $\Delta\rho_{ex}$ (red) is overwhelmed by ρ_{ex}^0 (dashed) unless $V_j \gg \gamma_j$.

In Fig 1b, we analyze the same system as Fig 1a in terms of light and matter DOS. For clarity, we consider $N = 4$ and $V_j = \gamma_{j(0)} = \Omega/4$, but in a realistic cavity, N is very large and $V_j \ll$

γ_j . The photonic DOS (blue) reveals two peaks that can be regarded as LP and UP, and the integral of each peak agrees with the expected Hopfield coefficient¹ of 1/2. The matter DOS (black) reveals DOS from LP and UP as well as the $N - 1$ dark states. The change in DOS (red) shows the redistribution of DOS compared to the unperturbed DOS (dashed). The DOS for the bright collective matter state can be obtained by considering a model with $N = 1$ and coupling g . In this simplified example, the bright matter DOS exactly matches $\rho_{ph}(\omega)$ (blue). Altogether we see that the DOS picture (Fig 1b) is consistent with discrete picture of polaritons (Fig. 1a).

Despite this consistency, the spectral broadening of $\rho_{ex}(\omega)$ (Fig. 1b) points to significant complications with the conventional analysis of bright and dark states. The set of 1 bright and $N - 1$ dark states represent the matter basis in which H is block diagonal. However, this basis only exists when all N matter states are perfectly degenerate. If the matter states lie on a distribution, which is true for realistic materials, then H cannot be block diagonalized and there are no longer any dark states. As a result, there is no good basis in which $\rho_{ex}(\omega)$ can be separated into bright and dark components. Although the positive peaks of $\Delta\rho_{ex}(\omega)$ seem to represent LP and UP, these peaks do not represent unique states that can be distinguished from $\rho_{ex}^0(\omega)$ unless $\Delta\rho_{ex}(\omega)$ and $\rho_{ex}^0(\omega)$ are spectrally separate. If $\Delta\rho_{ex}(\omega)$ and $\rho_{ex}^0(\omega)$ were spectrally separate, then the positive peaks of $\Delta\rho_{ex}(\omega)$ could be assigned to LP and UP, with the integral of each peak matching the Hopfield coefficient. However, such a regime is difficult to achieve. It may seem that spectral separation can be achieved by increasing N , which increases the peak separation of $\Delta\rho_{ex}(\omega)$. Unfortunately, increasing N also increases $\rho_{ex}^0(\omega)$ (Eq. 10) and so the spectral overlap remains. Spectral separation can only be achieved if $V_j \gg \gamma_j$, which is the criteria for single molecule strong

coupling. In realistic cavities, $V_j \ll \gamma_j$ and $\Delta\rho_{ex}(\omega)$ is barely perceptible relative to $\rho_{ex}^0(\omega)$ for large N . In this realistic regime, $\Delta\rho_{ex}(\omega)$ can essentially be neglected.

Since the matter DOS associated with $\rho_{ph}(\omega)$ is predominated by $\rho_{ex}^0(\omega)$, all the polaritons states should be viewed as gray states. We define gray states to be the collection of states with a matter DOS that scales with N . Gray states are intermediate between dark states, which scale with N but have no photonic character, and bright states, which have photonic character but do not scale with N . Conventionally, the matter fraction of LP and UP are extracted from measurements of the photonic DOS; however, defining the matter fraction in this way has no precise meaning. Instead, the photonic DOS is shared over a vast number of matter states. Overall, the continuum model, which includes spectral broadening, demonstrates complications with the standard polariton picture when N is large.

Self-energy relationship. The self-energy $\Sigma_0(\omega)$ is the essential quantity that dictates the light and matter DOS. Crucially, $\Sigma_0(\omega)$ is directly related to the refractive index n of the absorbing material. For the bare cavity, with refractive index n_0 , cavity confinement restricts wavenumber k to some discrete value k_0 , yielding a cavity mode with a resonance frequency ω_0 that satisfies $ck_0 = n_0\omega_0$, where c is the speed of light. After introducing an absorbing material, with additional refractive index Δn , the resonance frequency ω must satisfy $ck_0 = (n_0 + \Delta n)\omega$. Equating these relations, we find that ω must satisfy $\omega - \omega_0 + \omega \Delta n/n_0 = 0$, which is equivalent to the denominator of $G_{00}(\omega)$ provided that

$$\Sigma_0(\omega) = -\frac{\Delta n}{n_0}\omega. \quad (7)$$

Therefore, there is a simple, yet crucial, relationship between $\Sigma_0(\omega)$ and Δn .

This relationship can be demonstrated explicitly from the Lorentz oscillator model.³¹ For an absorbing material with susceptibility $\chi(\omega)$, the refractive index is $n(\omega) = \sqrt{\varepsilon_\infty + \chi(\omega)} \approx n_0 + \chi(\omega)/2n_0$, where it is assumed that $\chi(\omega) \ll \varepsilon_\infty$ and $n_0 = \sqrt{\varepsilon_\infty}$ is the refractive index of the bare cavity, which is approximated as a constant. The total susceptibility $\chi(\omega)$ of the absorbing material can be expressed as $\chi(\omega) = \int d\omega_j D(\omega_j) \chi_j(\omega)$ with $\chi_j(\omega)$ given by,

$$\chi_j(\omega) = \frac{\varepsilon_\infty \Omega_j^2}{\omega_j^2 - \omega^2 - i\gamma_j \omega} \approx \left(\frac{\varepsilon_\infty \Omega_j^2}{2\omega} \right) \frac{1}{\omega_j - \omega - i\gamma_j/2}, \quad (8)$$

where Ω_j parametrizes the oscillator strength of resonance j . In Eq. 8, we assume $|\omega_j - \omega| \ll \omega$ such that $\omega_j + \omega \approx 2\omega$, which is analogous to the rotating wave approximation.³² Using $\Delta n = \chi(\omega)/2n_0$, one finds that Eq. 7 is satisfied provided that $\sqrt{N}V_j = \Omega_j/2$. Thus Ω_j represents the collective Rabi splitting for N molecules each with coupling strength V_j . Therefore, using both a heuristic approach based on the dispersion relation and an explicit derivation using Lorentz oscillators, we have derived a key relationship between $\Sigma_0(\omega)$ and $\Delta n(\omega)$ (Eq. 7).

To understand the relationship between self-energy and refractive index, we will consider the modes of a simplified Fabry-Perot cavity. In Fig. 2a, we consider a bare cavity with index n_0 , which has a single cavity mode with frequency $\tilde{\omega}_0$. Introducing an absorbing material with a single resonance $\tilde{\omega}_j$, perturbs the refractive index to $n = n_0 + \Delta n$. Due to the modified dispersion relation, $ck_0 = n\omega$, there is a splitting of the mode, yielding UP and LP. Within the strong coupling regime, the mode splitting can be approximated as a coupling between light and matter oscillators (Fig. 2b). Using self-energy $\Sigma_0(\omega)$, the frequencies of LP and UP are given by solutions to $\omega = \tilde{\omega}_0 + \Sigma_0(\omega)$.

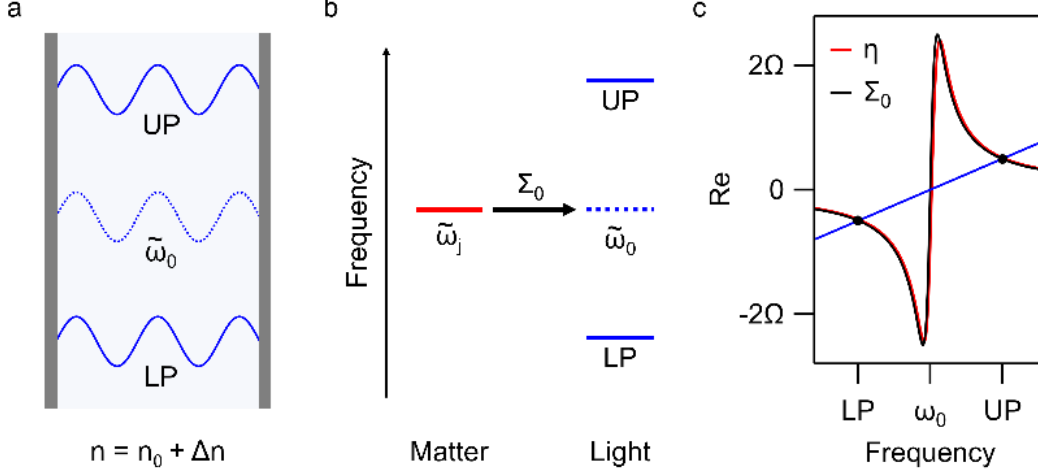


Figure 2. a) Simplified Fabry-Perot cavity, with cavity mode $\tilde{\omega}_0$ (dashed). The dispersion introduced by the absorber (Δn), produces a mode splitting into LP and UP (the spatial separation is illustrative). b) Coupled oscillator model of LP and UP, expressed in terms of Σ_0 . c) Graphical solution for LP and UP frequencies from the intersection of $\eta = -\omega \Delta n/n_0$ (red) or Σ_0 (black) with the line $\omega - \omega_0$ (blue). We consider $\omega_0 = \omega_j = 10\Omega$ and $\gamma_0 = \gamma_j = 0.1\Omega$.

For both approaches (Fig. 2a and 2b), the frequencies of UP and LP can be obtained graphically (Fig. 2c). Solutions to $ck_0 = n\omega$ occur at the intersection between $\omega - \omega_0$ (blue) and $\text{Re}[-\omega \Delta n/n_0]$ (red). Similarly, solutions to $\omega = \tilde{\omega}_0 + \Sigma_0$ occur at the intersection between $\omega - \omega_0$ (blue) and $\text{Re}[\Sigma_0(\omega)]$ (black). The corresponding imaginary parts of these functions provide the lifetimes of the modes. Even though the blue line intersects the functions at three points, the central intersection at ω_0 is neglected due to the low lifetime (i.e., a large imaginary part). For reasonable parameters, $-\omega \Delta n/n_0$ and $\Sigma_0(\omega)$ are nearly but not exactly equal.

Experimental modeling. The relationship between $\Delta n(\omega)$ and $\Sigma_0(\omega)$ enables the coupled oscillator model to be applied directly to experimental data, since $\Delta n(\omega)$ can be calculated from the absorption spectrum of the material of interest. As an example, we consider a cavity containing the dye Rhodamine 6G (R6G), which features an absorption spectrum with a peak centered at 530 nm and a shoulder around 500 nm (Fig. 3a, inset). The imaginary part of Δn is directly related to the molar absorbance $\varepsilon(\lambda)$ using $\text{Im}[\Delta n(\lambda)] = \ln(10) \lambda q \varepsilon(\lambda) / 4\pi$, where λ is the wavelength, and

q is the molar concentration. The real part of Δn can then be obtained from the imaginary part via the Kramers-Kronig relation (Fig. 3a). Invoking Eq. 7, $G_{00}(\omega)$ can be computed using

$$G_{00}(\omega) = \left[\left(1 + \frac{\Delta n(\omega)}{n_0} \right) \omega - \tilde{\omega}_0 \right]^{-1}, \quad (9)$$

and $\rho_{ph}(\omega)$ can be calculated from the imaginary part of Eq. 9. Here we consider ω in units of energy (eV) and convert from wavelength with $\omega = hc/\lambda$, where h is Planck's constant.

In Fig. 3b, we consider a cavity with a mode that is centered at $\lambda_0 = 530$ nm with a linewidth of $\gamma_0 = 100$ meV (black). Increasing the molar concentration of R6G from 0.0 M to 1.0 M results in an increased splitting in the photonic density of states (Fig. 3b). The upper peak exhibits changes in spectral shape with increasing R6G concentration due to the shoulder feature in the absorbance (Fig. 3a inset). Only when the concentration is high enough (e.g., 1.0 M, purple), such that the upper peak is above the absorption shoulder, does the upper peak assume a Lorentzian line shape. This phenomenon is consistent with the original analysis of inhomogeneous disorder which considered idealized Gaussian broadening.²⁴ Using Eq. 9, this analysis can be performed on any material with an arbitrary absorption spectrum.

We can additionally calculate $\Delta\rho_{ex}(\omega)$ from the absorption spectrum of the molecule. Applying Eq. 7 to Eq. 6, we derive

$$\Delta\rho_{ex}(\omega) = -\frac{1}{\pi} \text{Im} \left[\frac{\omega \Delta n'(\omega) + \Delta n(\omega)}{\omega n(\omega) - \tilde{\omega}_0 n_0} \right], \quad (10)$$

where $\Delta n'(\omega)$ denotes the derivative with respect to ω , and $n(\omega) = n_0 + \Delta n(\omega)$ represents the total refractive index. In Fig. 3c, $\Delta\rho_{ex}(\omega)$ for 0.1 M and 1.0 M R6G associated with Fig. 2b is presented. $\Delta\rho_{ex}(\omega)$ displays a complex spectral shape with a negative peak centered at the cavity

mode that is flanked by two positive peaks. The separation between the positive peaks increases with increasing concentration. While it is tempting to attribute the positive peaks to LP and UP, these positive peaks are negligible compared to $\rho_{ex}^0(\omega)$, and thus the polariton states should be viewed as gray states. Nonetheless, Eq. 10 provides a precise formula to compute the change in matter DOS due to light-matter coupling.

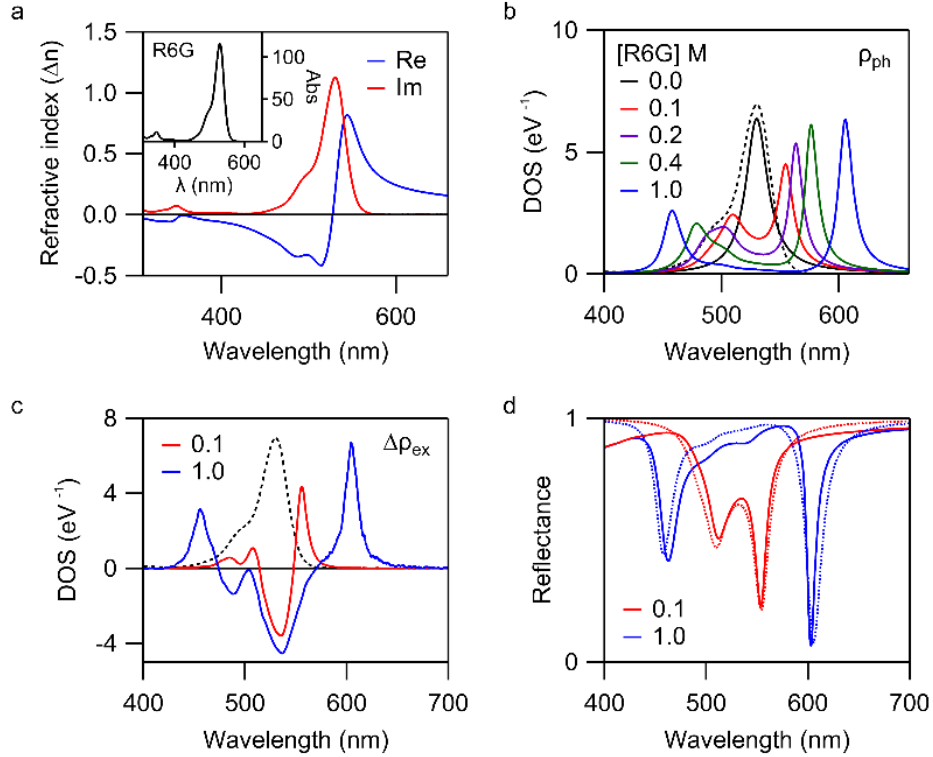


Figure 3. a) Refractive index for R6G (1.0 M) obtained from molar absorption spectrum (inset, $10^3 \text{ cm}^{-1}\text{M}^{-1}$). b) $\rho_{ph}(\omega)$ for a cavity ($\lambda_0 = 530 \text{ nm}$, $\gamma_0 = 100 \text{ meV}$) containing varying concentrations of R6G. c) $\Delta\rho_{ex}(\omega)$ associated with (b) for 0.1 M (red) or 1.0 M (blue) R6G. d) Modeled reflectance for the cavity structure: Ag (40 nm)/R6G (115 nm)/Ag (200 nm) using the Green's matrix (dashed) and the transfer matrix (solid) models with 0.1 M (red) or 1.0 M (blue) R6G.

The Green's matrix approach can also be used to compute scattering amplitudes, which are the main quantities that are measured experimentally.³³ For scattering off a single state (i.e., $G_{00}(\omega)$) in one dimension, the transmittance is $T(\omega) = \gamma_a \gamma_b |G_{00}(\omega)|^2$ and the reflectance is

$R(\omega) = |1 - i\gamma_a G_{00}(\omega)|^2$, where γ_a and γ_b denote the incoming and outgoing couplings, respectively.³⁴ These couplings contribute to the cavity mode loss $\gamma_0 = \gamma_a + \gamma_b + \gamma_c$, where γ_c accounts for absorption by the cavity. For a Fabry-Perot cavity, γ_0 can be estimated using $R_a R_b = e^{-\gamma_0 \tau_0}$, where $R_{a(b)}$ are the reflectance of the mirrors and $\tau_0 = 2Ln_0/c$ is the round-trip time for a cavity of length L . Similarly, $\gamma_{a(b)}$ can be approximated using $T_{a(b)} = 1 - e^{-\gamma_{a(b)} \tau_0} \approx \gamma_{a(b)} \tau_0$, where $T_{a(b)}$ are the mirror transmittances which are assumed to be small. Using these relations, we find good agreement between the Green's matrix approach and the transfer matrix method for a characteristic silver cavity containing either low or high concentrations of R6G (Fig. 3d). This agreement can also be demonstrated explicitly. For example, the transmittance through a Fabry-Perot cavity is given by $T(\omega) = |t_a t_b e^{i\omega\tau/2} / (1 - r_a r_b e^{i\omega\tau})|^2$, where $t_{a(b)}$ and $r_{a(b)}$ are the transmission and reflection coefficients of the mirrors, and $\tau = 2Ln/c = (1 + \Delta n/n_0)\tau_0$ is the round-trip time in the cavity. Close to the cavity resonance ω_0 , expanding the exponential in the denominator to first order and neglecting the imaginary part of Δn in the numerator, yields $T(\omega) = \gamma_a \gamma_b |G_{00}(\omega)|^2$. Therefore, $\Sigma_0(E)$ reveals an explicit connection between scattering measurements and the coupled oscillator model.

CONCLUSIONS

The linear light-matter interaction in a material is defined by its refractive index. We derive the fundamental relationship between this refractive index and the polariton formalism, which expresses the light-matter interaction in terms of coupled light and matter states. Using this relationship, we present a generalized model of polaritons that can be applied to materials with complex absorption spectra, including organic molecules as well as inorganic materials such as perovskites.³⁵ We demonstrate that the light and matter DOS can be calculated directly from the

measured absorption spectra, enabling precise analysis of polariton states. The photonic DOS displays a broad spectral distribution that only approaches the discrete polariton picture when the peak splitting exceeds the breadth of the absorption peak. The matter DOS exhibits a change in DOS that is small compared to the total DOS. This change in matter DOS cannot be meaningfully assigned to bright states that are partitioned from a reservoir of dark states. Instead, all the polariton states should be regarded as gray states, in which limited photonic character is shared between a large number of primarily matter excitations. This picture could have profound implications for the interpretation of polariton chemistry and photophysics, as the photonic content of the states directly impacts key properties like lifetime and the distortion of the potential energy surface. With more precise models of polaritons, that are informed by experimental data, we expect an improved understanding of molecular polariton phenomena such as enhanced energy transport and modified reactivity.

ACKNOWLEDGMENTS

S.G. acknowledges support from the Arnold O. Beckman Postdoctoral Fellowship in Chemical Instrumentation and former support from the National Science Foundation under Grant # EEC-2127509 to the American Society for Engineering Education. R.F.P. acknowledges support from the Nexus Scholars Program at Cornell University. A.J.M. acknowledge support by the U.S. Department of Energy, Office of Science, Basic Energy Sciences, CPIMS Program under Early Career Research Program (Award No. DE-SC0021941).

REFERENCES

- (1) Hopfield, J. J. Theory of the Contribution of Excitons to the Complex Dielectric Constant of Crystals. *Phys. Rev.* **1958**, *112* (5), 1555–1567. <https://doi.org/10.1103/PhysRev.112.1555>.
- (2) Mills, D. L.; Burstein, E. Polaritons: The Electromagnetic Modes of Media. *Rep. Prog. Phys.* **1974**, *37* (7), 817. <https://doi.org/10.1088/0034-4885/37/7/001>.

- (3) Jaynes, E. T.; Cummings, F. W. Comparison of Quantum and Semiclassical Radiation Theories with Application to the Beam Maser. *Proc. IEEE* **1963**, *51* (1), 89–109. <https://doi.org/10.1109/PROC.1963.1664>.
- (4) Tavis, M.; Cummings, F. W. Exact Solution for an N -Molecule—Radiation-Field Hamiltonian. *Phys. Rev.* **1968**, *170* (2), 379–384. <https://doi.org/10.1103/PhysRev.170.379>.
- (5) *Microcavities*, Second Edition.; Kavokin, A., Ed.; Series on semiconductor science and technology; Oxford University Press: Oxford ; New York, NY, 2017.
- (6) Ebbesen, T. W. Hybrid Light–Matter States in a Molecular and Material Science Perspective. *Acc. Chem. Res.* **2016**, *49* (11), 2403–2412. <https://doi.org/10.1021/acs.accounts.6b00295>.
- (7) Balasubrahmaniyam, M.; Simkhovich, A.; Golombek, A.; Sandik, G.; Ankonina, G.; Schwartz, T. From Enhanced Diffusion to Ultrafast Ballistic Motion of Hybrid Light–Matter Excitations. *Nat. Mater.* **2023**, *22* (3), 338–344. <https://doi.org/10.1038/s41563-022-01463-3>.
- (8) Coles, D. M.; Somaschi, N.; Michetti, P.; Clark, C.; Lagoudakis, P. G.; Savvidis, P. G.; Lidzey, D. G. Polariton-Mediated Energy Transfer between Organic Dyes in a Strongly Coupled Optical Microcavity. *Nat. Mater.* **2014**, *13* (7), 712–719. <https://doi.org/10.1038/nmat3950>.
- (9) Xiang, B.; Ribeiro, R. F.; Du, M.; Chen, L.; Yang, Z.; Wang, J.; Yuen-Zhou, J.; Xiong, W. Intermolecular Vibrational Energy Transfer Enabled by Microcavity Strong Light–Matter Coupling. *Science* **2020**, *368* (6491), 665–667. <https://doi.org/10.1126/science.aba3544>.
- (10) Orgiu, E.; George, J.; Hutchison, J. A.; Devaux, E.; Dayen, J. F.; Doudin, B.; Stellacci, F.; Genet, C.; Schachenmayer, J.; Genes, C.; Pupillo, G.; Samorì, P.; Ebbesen, T. W. Conductivity in Organic Semiconductors Hybridized with the Vacuum Field. *Nat. Mater.* **2015**, *14* (11), 1123–1129. <https://doi.org/10.1038/nmat4392>.
- (11) Krainova, N.; Grede, A. J.; Tsokkou, D.; Banerji, N.; Giebink, N. C. Polaron Photoconductivity in the Weak and Strong Light-Matter Coupling Regime. *Phys. Rev. Lett.* **2020**, *124* (17), 177401. <https://doi.org/10.1103/PhysRevLett.124.177401>.
- (12) Kéna-Cohen, S.; Forrest, S. R. Room-Temperature Polariton Lasing in an Organic Single-Crystal Microcavity. *Nat. Photonics* **2010**, *4* (6), 371–375. <https://doi.org/10.1038/nphoton.2010.86>.
- (13) Plumhof, J. D.; Stöferle, T.; Mai, L.; Scherf, U.; Mahrt, R. F. Room-Temperature Bose–Einstein Condensation of Cavity Exciton–Polaritons in a Polymer. *Nat. Mater.* **2014**, *13* (3), 247–252. <https://doi.org/10.1038/nmat3825>.
- (14) Thomas, A.; Lethuillier-Karl, L.; Nagarajan, K.; Vergauwe, R. M. A.; George, J.; Chervy, T.; Shalabney, A.; Devaux, E.; Genet, C.; Moran, J.; Ebbesen, T. W. Tilting a Ground-State Reactivity Landscape by Vibrational Strong Coupling. *Science* **2019**, *363* (6427), 615–619. <https://doi.org/10.1126/science.aau7742>.
- (15) Ahn, W.; Triana, J. F.; Recabal, F.; Herrera, F.; Simpkins, B. S. Modification of Ground-State Chemical Reactivity via Light–Matter Coherence in Infrared Cavities. *Science* **2023**, *380* (6650), 1165–1168. <https://doi.org/10.1126/science.ade7147>.
- (16) Chen, T.-T.; Du, M.; Yang, Z.; Yuen-Zhou, J.; Xiong, W. Cavity-Enabled Enhancement of Ultrafast Intramolecular Vibrational Redistribution over Pseudorotation. *Science* **2022**, *378* (6621), 790–794. <https://doi.org/10.1126/science.add0276>.
- (17) Haroche, S.; Kleppner, D. Cavity Quantum Electrodynamics. *Phys. Today* **1989**, *42* (1), 24–30. <https://doi.org/10.1063/1.881201>.

- (18) Skolnick, M. S.; Fisher, T. A.; Whittaker, D. M. Strong Coupling Phenomena in Quantum Microcavity Structures. *Semicond. Sci. Technol.* **1998**, *13* (7), 645. <https://doi.org/10.1088/0268-1242/13/7/003>.
- (19) Son, M.; Armstrong, Z. T.; Allen, R. T.; Dhavamani, A.; Arnold, M. S.; Zanni, M. T. Energy Cascades in Donor-Acceptor Exciton-Polaritons Observed by Ultrafast Two-Dimensional White-Light Spectroscopy. *Nat. Commun.* **2022**, *13* (1), 7305. <https://doi.org/10.1038/s41467-022-35046-2>.
- (20) Engelhardt, G.; Cao, J. Unusual Dynamical Properties of Disordered Polaritons in Microcavities. *Phys. Rev. B* **2022**, *105* (6), 064205. <https://doi.org/10.1103/PhysRevB.105.064205>.
- (21) Gera, T.; Sebastian, K. L. Effects of Disorder on Polaritonic and Dark States in a Cavity Using the Disordered Tavis–Cummings Model. *J. Chem. Phys.* **2022**, *156* (19), 194304. <https://doi.org/10.1063/5.0086027>.
- (22) Gera, T.; Sebastian, K. L. Exact Results for the Tavis–Cummings and Hückel Hamiltonians with Diagonal Disorder. *J. Phys. Chem. A* **2022**. <https://doi.org/10.1021/acs.jpca.2c02359>.
- (23) Whittaker, D. M. What Determines Inhomogeneous Linewidths in Semiconductor Microcavities? *Phys. Rev. Lett.* **1998**, *80* (21), 4791–4794. <https://doi.org/10.1103/PhysRevLett.80.4791>.
- (24) Houdré, R.; Stanley, R. P.; Ilegems, M. Vacuum-Field Rabi Splitting in the Presence of Inhomogeneous Broadening: Resolution of a Homogeneous Linewidth in an Inhomogeneously Broadened System. *Phys. Rev. A* **1996**, *53* (4), 2711–2715. <https://doi.org/10.1103/PhysRevA.53.2711>.
- (25) Litinskaya, M.; Reineker, P. Loss of Coherence of Exciton Polaritons in Inhomogeneous Organic Microcavities. *Phys. Rev. B* **2006**, *74* (16), 165320. <https://doi.org/10.1103/PhysRevB.74.165320>.
- (26) Newns, D. M. Self-Consistent Model of Hydrogen Chemisorption. *Phys. Rev.* **1969**, *178* (3), 1123–1135. <https://doi.org/10.1103/PhysRev.178.1123>.
- (27) Anderson, P. W. Localized Magnetic States in Metals. *Phys. Rev.* **1961**, *124* (1), 41–53. <https://doi.org/10.1103/PhysRev.124.41>.
- (28) Grimley, T. B. The Electron Density in a Metal near a Chemisorbed Atom or Molecule. *Proc. Phys. Soc.* **1967**, *92* (3), 776. <https://doi.org/10.1088/0370-1328/92/3/329>.
- (29) Romero, M. A.; Goldberg, E. C. Local Density of States of Atoms Interacting with Finite-Bandwidth Surfaces: Spin-Statistics Effects. *Phys. Rev. B* **2006**, *74* (19), 195419. <https://doi.org/10.1103/PhysRevB.74.195419>.
- (30) Du, M.; Poh, Y. R.; Yuen-Zhou, J. Vibropolaritonic Reaction Rates in the Collective Strong Coupling Regime: Pollak–Grabert–Hänggi Theory. *J. Phys. Chem. C* **2023**, *127* (11), 5230–5237. <https://doi.org/10.1021/acs.jpcc.3c00122>.
- (31) Klingshirn, C. F. *Semiconductor Optics*; Springer: Berlin Heidelberg New York, 1995.
- (32) Snoke, D. W. *Solid State Physics: Essential Concepts*, Second edition.; Cambridge University Press: Cambridge, United Kingdom ; New York, NY, 2019.
- (33) F. Ribeiro, R.; Dunkelberger, A. D.; Xiang, B.; Xiong, W.; Simpkins, B. S.; Owrutsky, J. C.; Yuen-Zhou, J. Theory for Nonlinear Spectroscopy of Vibrational Polaritons. *J. Phys. Chem. Lett.* **2018**, *9* (13), 3766–3771. <https://doi.org/10.1021/acs.jpcclett.8b01176>.

- (34) Cuevas, J. C.; Scheer, E. *Molecular Electronics: An Introduction to Theory and Experiment*; World Scientific series in nanoscience and nanotechnology; World Scientific: Singapore ; Hackensack, NJ, 2010.
- (35) Xu, D.; Mandal, A.; Baxter, J. M.; Cheng, S.-W.; Lee, I.; Su, H.; Liu, S.; Reichman, D. R.; Delor, M. Ultrafast Imaging of Polariton Propagation and Interactions. *Nat. Commun.* **2023**, *14* (1), 3881. <https://doi.org/10.1038/s41467-023-39550-x>.